

**Observation of a $p\bar{p}$ mass threshold enhancement in
 $\psi' \rightarrow \pi^+\pi^-J/\psi(J/\psi \rightarrow \gamma p\bar{p})$ decay**

M. Ablikim¹, M. N. Achasov⁵, L. An⁹, Q. An³¹, Z. H. An¹, J. Z. Bai¹, Y. Ban¹⁸, N. Berger¹, J. M. Bian¹, I. Boyko¹³, R. A. Briere³, V. Bytev¹³, X. Cai¹, G. F. Cao¹, X. X. Cao¹, J. F. Chang¹, G. Chelkov^{13a}, G. Chen¹, H. S. Chen¹, J. C. Chen¹, L. P. Chen¹, M. L. Chen¹, P. Chen¹, S. J. Chen¹⁶, Y. B. Chen¹, Y. P. Chu¹, D. Cronin-Hennessy³⁰, H. L. Dai¹, J. P. Dai¹, D. Dedovich¹³, Z. Y. Deng¹, I. Denysenko^{13b}, M. Destefanis³², Y. Ding¹⁴, L. Y. Dong¹, M. Y. Dong¹, S. X. Du³⁶, M. Y. Duan²¹, J. Fang¹, C. Q. Feng³¹, C. D. Fu¹, J. L. Fu¹⁶, Y. Gao²⁷, C. Geng³¹, K. Goetzen⁷, W. X. Gong¹, M. Greco³², S. Grishin¹³, Y. T. Gu⁹, A. Q. Guo¹⁷, L. B. Guo¹⁵, Y. P. Guo¹⁷, S. Q. Han¹⁵, F. A. Harris²⁹, K. L. He¹, M. He¹, Z. Y. He¹⁷, Y. K. Heng¹, Z. L. Hou¹, H. M. Hu¹, J. F. Hu⁶, T. Hu¹, X. W. Hu¹⁶, B. Huang¹, G. M. Huang¹¹, J. S. Huang¹⁰, X. T. Huang²⁰, Y. P. Huang¹, C. S. Ji³¹, Q. Ji¹, X. B. Ji¹, X. L. Ji¹, L. K. Jia¹, L. L. Jiang¹, X. S. Jiang¹, J. B. Jiao²⁰, D. P. Jin¹, S. Jin¹, S. Komamiya²⁶, W. Kuehn²⁸, S. Lange²⁸, J. K. C. Leung²⁵, Cheng Li³¹, Cui Li³¹, D. M. Li³⁶, F. Li¹, G. Li¹, H. B. Li¹, J. Li¹, J. C. Li¹, Lei Li¹, Lu Li¹, Q. J. Li¹, W. D. Li¹, W. G. Li¹, X. L. Li²⁰, X. N. Li¹, X. Q. Li¹⁷, X. R. Li¹, Y. X. Li³⁶, Z. B. Li²³, H. Liang³¹, T. R. Liang¹⁷, Y. L. Liang²⁸, Y. F. Liang²², G. R. Liao⁸, X. T. Liao¹, B. J. Liu^{24,25}, C. L. Liu³, C. X. Liu¹, C. Y. Liu¹, F. H. Liu²¹, Fang Liu¹, Feng Liu¹¹, G. C. Liu¹, H. Liu¹, H. B. Liu⁶, H. M. Liu¹, H. W. Liu¹, J. Liu¹, J. P. Liu³⁴, K. Liu¹⁸, K. Y. Liu¹⁴, Q. Liu²⁹, S. B. Liu³¹, X. H. Liu¹, Y. B. Liu¹⁷, Y. F. Liu¹⁷, Y. W. Liu³¹, Yong Liu¹, Z. A. Liu¹, G. R. Lu¹⁰, J. G. Lu¹, Q. W. Lu²¹, X. R. Lu⁶, Y. P. Lu¹, C. L. Luo¹⁵, M. X. Luo³⁵, T. Luo¹, X. L. Luo¹, C. L. Ma⁶, F. C. Ma¹⁴, H. L. Ma¹, Q. M. Ma¹, X. Ma¹, X. Y. Ma¹, M. Maggiora³², Y. J. Mao¹⁸, Z. P. Mao¹, J. Min¹, X. H. Mo¹, N. Yu. Muchnoi⁵, Y. Nefedov¹³, F. P. Ning²¹, S. L. Olsen¹⁹, Q. Ouyang¹, M. Pelizaeus², K. Peters⁷, J. L. Ping¹⁵, R. G. Ping¹, R. Poling³⁰, C. S. J. Pun²⁵, M. Qi¹⁶, S. Qian¹, C. F. Qiao⁶, J. F. Qiu¹, G. Rong¹, X. D. Ruan⁹, A. Sarantsev^{13c}, M. Shao³¹, C. P. Shen²⁹, X. Y. Shen¹, H. Y. Sheng¹, S. Sonoda²⁶, S. Spataro³², B. Spruck²⁸, D. H. Sun¹, G. X. Sun¹, J. F. Sun¹⁰, S. S. Sun¹, X. D. Sun¹, Y. J. Sun³¹, Y. Z. Sun¹, Z. J. Sun¹, Z. T. Sun³¹, C. J. Tang²², X. Tang¹, X. F. Tang⁸, H. L. Tian¹, D. Toth³⁰, G. S. Varner²⁹, X. Wan¹, B. Q. Wang¹⁸, J. K. Wang¹, K. Wang¹, L. L. Wang⁴, L. S. Wang¹, P. Wang¹, P. L. Wang¹, Q. Wang¹, S. G. Wang¹⁸, X. D. Wang²¹, X. L. Wang³¹, Y. D. Wang³¹, Y. F. Wang¹, Y. Q. Wang²⁰, Z. Wang¹, Z. G. Wang¹, Z. Y. Wang¹, D. H. Wei⁸, S. P. Wen¹, U. Wiedner², L. H. Wu¹, N. Wu¹, Y. M. Wu¹, Z. Wu¹, Z. J. Xiao¹⁵, Y. G. Xie¹, G. F. Xu¹, G. M. Xu¹⁸, H. Xu¹, Min Xu³¹, Ming Xu⁹, X. P. Xu^{11d}, Y. Xu¹⁷, Z. Z. Xu³¹, Z. Xue³¹, L. Yan³¹, W. B. Yan³¹, Y. H. Yan¹², H. X. Yang¹, M. Yang¹, P. Yang¹⁷, S. M. Yang¹, Y. X. Yang⁸, M. Ye¹, M. H. Ye⁴, B. X. Yu¹, C. X. Yu¹⁷, L. Yu¹¹, C. Z. Yuan¹, Y. Yuan¹, Y. Zeng¹², B. X. Zhang¹, B. Y. Zhang¹, C. C. Zhang¹, D. H. Zhang¹, H. H. Zhang²³, H. Y. Zhang¹, J. W. Zhang¹, J. Y. Zhang¹, J. Z. Zhang¹, L. Zhang¹⁶, S. H. Zhang¹, X. Y. Zhang²⁰, Y. Zhang¹, Y. H. Zhang¹, Z. P. Zhang³¹, C. Zhao³¹, H. S. Zhao¹, Jiawei Zhao³¹, Jingwei Zhao¹, Lei Zhao³¹, Ling Zhao¹, M. G. Zhao¹⁷, Q. Zhao¹, S. J. Zhao³⁶, T. C. Zhao³³, X. H. Zhao¹⁶, Y. B. Zhao¹, Z. G. Zhao³¹, A. Zhemchugov^{13a}, B. Zheng¹, J. P. Zheng¹, Y. H. Zheng⁶, Z. P. Zheng¹, B. Zhong¹⁵, J. Zhong², L. Zhou¹, Z. L. Zhou¹, C. Zhu¹, K. Zhu¹, K. J. Zhu¹, Q. M. Zhu¹, X. W. Zhu¹, Y. S. Zhu¹, Z. A. Zhu¹, J. Zhuang¹, B. S. Zou¹, J. H. Zou¹, J. X. Zuo¹, P. Zweber³⁰

(BESIII Collaboration)

¹ *Institute of High Energy Physics, Beijing 100049, P. R. China*

² *Bochum Ruhr-University, 44780 Bochum, Germany*

³ *Carnegie Mellon University, Pittsburgh, PA 15213, USA*

⁴ *China Center of Advanced Science and Technology, Beijing 100190, P. R. China*

⁵ *G.I. Budker Institute of Nuclear Physics SB RAS (BINP), Novosibirsk 630090, Russia*

⁶ *Graduate University of Chinese Academy of Sciences, Beijing 100049, P. R. China*

⁷ *GSI Helmholtzcentre for Heavy Ion Research GmbH, D-64291 Darmstadt, Germany*

⁸ *Guangxi Normal University, Guilin 541004, P. R. China*

⁹ *Guangxi University, Nanning 530004, P. R. China*

¹⁰ *Henan Normal University, Xinxiang 453007, P. R. China*

¹¹ *Huazhong Normal University, Wuhan 430079, P. R. China*

¹² *Hunan University, Changsha 410082, P. R. China*

¹³ *Joint Institute for Nuclear Research, 141980 Dubna, Russia*

¹⁴ *Liaoning University, Shenyang 110036, P. R. China*

¹⁵ *Nanjing Normal University, Nanjing 210046, P. R. China*

¹⁶ *Nanjing University, Nanjing 210093, P. R. China*

- ¹⁷ Nankai University, Tianjin 300071, P. R. China
¹⁸ Peking University, Beijing 100871, P. R. China
¹⁹ Seoul National University, Seoul, 151-747 Korea
²⁰ Shandong University, Jinan 250100, P. R. China
²¹ Shanxi University, Taiyuan 030006, P. R. China
²² Sichuan University, Chengdu 610064, P. R. China
²³ Sun Yat-Sen University, Guangzhou 510275, P. R. China
²⁴ The Chinese University of Hong Kong, Shatin, N.T., Hong Kong.
²⁵ The University of Hong Kong, Pokfulam, Hong Kong
²⁶ The University of Tokyo, Tokyo 113-0033 Japan
²⁷ Tsinghua University, Beijing 100084, P. R. China
²⁸ Universitaet Giessen, 35392 Giessen, Germany
²⁹ University of Hawaii, Honolulu, Hawaii 96822, USA
³⁰ University of Minnesota, Minneapolis, MN 55455, USA
³¹ University of Science and Technology of China, Hefei 230026, P. R. China
³² University of Turin and INFN, Turin, Italy
³³ University of Washington, Seattle, WA 98195, USA
³⁴ Wuhan University, Wuhan 430072, P. R. China
³⁵ Zhejiang University, Hangzhou 310027, P. R. China
³⁶ Zhengzhou University, Zhengzhou 450001, P. R. China
^a also at the Moscow Institute of Physics and Technology, Moscow, Russia
^b on leave from the Bogolyubov Institute for Theoretical Physics, Kiev, Ukraine
^c also at the PNPI, Gatchina, Russia
^d currently at Suzhou University, Suzhou 215006, P. R. China

(Dated: January 29, 2010)

The decay channel $\psi' \rightarrow \pi^+\pi^- J/\psi (J/\psi \rightarrow \gamma p\bar{p})$ is studied using a sample of 1.06×10^8 ψ' events collected by the BESIII experiment at BEPCII. A strong enhancement at threshold is observed in the $p\bar{p}$ invariant mass spectrum. The enhancement can be fit with an S -wave Breit-Wigner resonance function with a resulting peak mass of $M = 1861^{+6}_{-13}$ (stat) $^{+7}_{-26}$ (syst) MeV/ c^2 and a narrow width that is $\Gamma < 38$ MeV/ c^2 at the 90% confidence level. These results are consistent with published BESII results. These mass and width values do not match with those of any known meson resonance.

PACS numbers: 13.85.Hd, 25.75.Gz

An anomalously strong $p\bar{p}$ mass threshold enhancement was observed by the BESII experiment in the radiative decay process $J/\psi \rightarrow \gamma p\bar{p}$ [1]. In ref. [1] it was noted that when an S -wave Breit-Wigner resonance function is fitted to the $p\bar{p}$ mass distribution, the peak mass is below the $p\bar{p}$ mass threshold at $M = 1859^{+3}_{-10}$ (stat) $^{+5}_{-25}$ (syst) MeV/ c^2 and the total width is $\Gamma < 30$ MeV/ c^2 (at the 90% C.L.). An interesting feature of this enhancement is that corresponding structures are not observed in near-threshold $p\bar{p}$ cross section measurements, in B -meson decays [2, 3], in radiative ψ' or $\Upsilon \rightarrow \gamma p\bar{p}$ decays [4, 5], or in $J/\psi \rightarrow \omega p\bar{p}$ decays [6]. These non-observations disfavor the attribution of the mass-threshold enhancement, which is uniquely observed in the $J/\psi \rightarrow \gamma p\bar{p}$ decay process, to the pure effects of $p\bar{p}$ final state interactions (FSI).

This experimental observation stimulated a number of theoretical speculations [7, 8, 9, 10, 11, 12]. One of these is the intriguing suggestion that it is an example of a $p\bar{p}$ bound state, sometimes called baryonium [13], which has a long history and has been the subject of many experimental searches [14].

In this letter we report a study of the $p\bar{p}$ mass spectrum in the threshold region in the decay process $\psi' \rightarrow \pi^+\pi^- J/\psi (J/\psi \rightarrow \gamma p\bar{p})$. The analysis uses a sample of 1.06×10^8 ψ' events accumulated by the upgraded Beijing Spectrometer (BESIII) located at the Beijing Electron-Positron Collider (BEPCII) at the Beijing Institute of High Energy Physics.

BEPCII/BESIII [15] is a major upgrade of the BESII experiment at the BEPC accelerator [16]. The design peak luminosity of the double-ring e^+e^- collider, BEPCII, is 10^{33} cm $^{-2}$ s $^{-1}$ at a beam current of 0.93 A. The BESIII detector with a geometrical acceptance of 93% of 4π , consists of the following main components: 1) a small-celled, helium-based main draft chamber (MDC) with 43 layers. The average single wire resolution is 135 μ m, and the momentum resolution for 1 GeV charged particles in a 1 T magnetic field is 0.5%; 2) an electromagnetic calorimeter (EMC) made of 6240 CsI (TI) crystals arranged in a cylindrical shape (barrel) plus two endcaps. For 1.0 GeV photons, the energy resolution is 2.5% in the barrel and 5% in the endcaps, and the position resolution is 6 mm in the barrel and 9 mm in the endcaps; 3) a

Time-Of-Flight system (TOF) for particle identification composed of a barrel part made of two layers with 88 pieces of 5 cm thick, 2.4 m long plastic scintillators in each layer, and two endcaps with 96 fan-shaped, 5 cm thick, plastic scintillators in each endcap. The time resolution is 80 ps in the barrel, and 110 ps in the endcaps, corresponding to a 2σ K/π separation for momenta up to about 1.0 GeV; 4) a muon chamber system (MUC) made of 1000 m² of Resistive Plate Chambers (RPC) arranged in 9 layers in the barrel and 8 layers in the endcaps and incorporated in the return iron of the superconducting magnet. The position resolution is about 2 cm.

Candidate $\psi' \rightarrow \pi^+\pi^-J/\psi$ ($J/\psi \rightarrow \gamma p\bar{p}$) events are required to have at least one photon and four charged tracks within the polar angle region $|\cos\theta| < 0.93$ and a total net charge of zero. The TOF and dE/dx information are combined to form particle identification confidence levels for the π , K , and p hypotheses; each track is assigned to the particle type that corresponds to the hypothesis with the highest confidence level. Selected events are required to have both an identified proton and an identified anti-proton and no particle identification is required for the two remaining tracks. Candidate photons are required to have an energy deposit that is at least 25 MeV in the barrel EMC ($|\cos\theta| < 0.8$) and 50 MeV in the endcap EMCs ($0.86 < |\cos\theta| < 0.92$), and be isolated from the anti-proton track by more than 30° due to the strong annihilation of anti-protons, and from all other charged tracks by more than 10° . EMC timing requirements suppress electronic noise and energy deposits unrelated to the event.

Candidate J/ψ signals are identified by the invariant mass recoiling against the $\pi^+\pi^-$ pair, $|M_{\pi^+\pi^-} - m_{J/\psi}| < 0.006$ GeV/ c^2 . Further requirements of $|U_{miss}| < 0.05$ GeV, where $U_{miss} = (E_{miss} - |P_{miss}|)$, and $P_{\gamma}^2 < 0.0005$ (GeV/ c)², where $P_{\gamma}^2 = 4|P_{miss}|^2 \sin^2\theta_\gamma/2$, are imposed to suppress backgrounds from multi-photon events. Here E_{miss} and P_{miss} are, respectively, the missing energy and momentum of all charged particles, and θ_γ is the angle between the missing momentum and the photon direction. The requirement $|M_{\pi^+\pi^-p\bar{p}} - m_{\psi'}| > 0.03$ GeV/ c^2 is used to reduce the background from $\psi' \rightarrow \pi^+\pi^-p\bar{p}$.

Events that remain after these selection requirements are subjected to a four-constraint energy-momentum conservation kinematic fit to the hypothesis $\psi' \rightarrow \gamma\pi^+\pi^-p\bar{p}$. For events with more than one γ candidate, the combination with the smallest χ^2 is chosen. Events with $\chi^2 < 100$ are selected. Since the detection efficiencies for data and Monte Carlo (MC) simulated events are consistent for protons and antiprotons with momenta $p > 0.3$ GeV/ c , while differences occur for lower momentum tracks, we reject events with $p_p < 0.3$ GeV/ c or $p_{\bar{p}} < 0.3$ GeV/ c .

Fig. 1(a) shows the $p\bar{p}$ invariant mass distribution for surviving events. The distribution features a peak near $M_{p\bar{p}} = 2.98$ GeV/ c^2 that is consistent in mass, width, and yield with expectations for $\psi' \rightarrow \pi^+\pi^-J/\psi$ ($J/\psi \rightarrow$

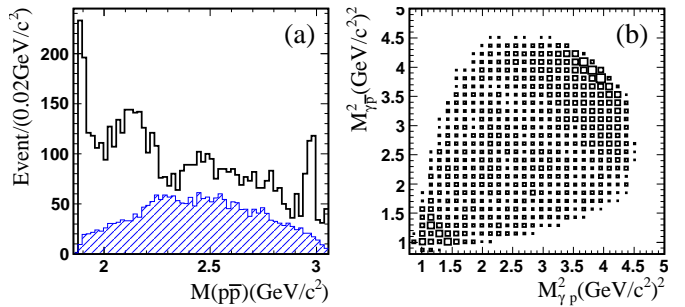


FIG. 1: The $p\bar{p}$ invariant mass spectrum for the selected $\psi' \rightarrow \pi^+\pi^-J/\psi$ ($J/\psi \rightarrow \gamma p\bar{p}$) candidate events. (a) The $p\bar{p}$ invariant mass spectrum; the open histogram is data and the hatched histogram is from a $\psi' \rightarrow \pi^+\pi^-J/\psi$ ($J/\psi \rightarrow \gamma p\bar{p}$) phase-space MC events (with arbitrary normalization). (b) An $M^2(\gamma p)$ (horizontal) versus $M^2(\gamma \bar{p})$ (vertical) Dalitz plot for the selected events.

$\gamma\eta_c, \eta_c \rightarrow p\bar{p}$), a broad enhancement around $M_{p\bar{p}} \sim 2.2$ GeV/ c^2 , and a prominent low-mass peak at the $p\bar{p}$ mass threshold, similar to that reported by BESII [1]. The Dalitz plot for selected events is shown in Fig. 1(b), where a band corresponding to the threshold enhancement is evident in the upper right corner.

Potential background processes are studied with an inclusive MC sample of 1×10^8 ψ' events generated according to the Lund-Charm model [17] and the Particle Data Group (PDG) decay tables [18]. None of background sources produce an enhancement at the threshold region of $p\bar{p}$ invariant-mass spectrum. The dominant background is from $\psi' \rightarrow \pi^+\pi^-J/\psi$ ($J/\psi \rightarrow \pi^0 p\bar{p}$) events, with asymmetric $\pi^0 \rightarrow \gamma\gamma$ decays where one of the photons has most of the π^0 energy. An exclusive MC sample of $\psi' \rightarrow \pi^+\pi^-J/\psi$ ($J/\psi \rightarrow \pi^0 p\bar{p}$), generated with a uniform phase space distribution, indicates that the level of this background in the selected event sample with $M_{p\bar{p}} - 2m_p < 0.3$ GeV/ c^2 is 9% of the total.

To ensure further that the $p\bar{p}$ threshold enhancement is not due to background, each potential background is studied with data. Non- J/ψ background are studied using J/ψ mass-sideband events. For these there is no enhancement and their level of contamination of the selected event sample is about 2%. The dominant background channel, $\psi' \rightarrow \pi^+\pi^-J/\psi$ ($J/\psi \rightarrow \pi^0 p\bar{p}$), is also studied with data. In this case, events with four charged tracks, including a proton and antiproton and two oppositely charged pions, and with two or more photons are selected, and subjected to a four-constraint kinematic fit to the $\psi' \rightarrow \gamma\gamma\pi^+\pi^-p\bar{p}$ hypothesis. J/ψ and π^0 signals are selected by the requirements $|M_{\pi^+\pi^-} - m_{J/\psi}| < 0.006$ GeV/ c^2 and $|M_{\gamma\gamma} - m_{\pi^0}| < 0.008$ GeV/ c^2 ($\pm 2\sigma$). There is no evidence of a narrow and strong enhancement near $p\bar{p}$ mass threshold region.

The $M_{p\bar{p}}$ invariant mass spectrum in the threshold region for the selected $\pi^0 p\bar{p}$ events is shown in Fig. 2(a), where no threshold enhancement is evident. The dis-

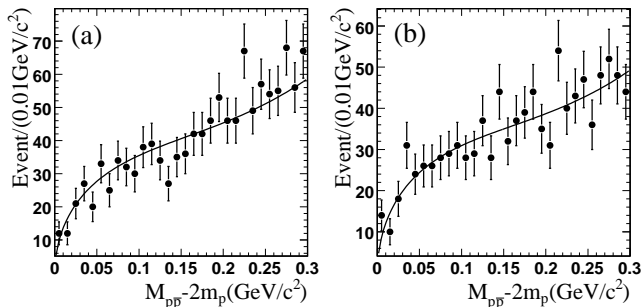


FIG. 2: The $p\bar{p}$ mass spectrum near threshold for: (a) selected $\psi' \rightarrow \pi^+\pi^- J/\psi (J/\psi \rightarrow \pi^0 p\bar{p})$ events for the same real data sample. (b) phase-space MC $\psi' \rightarrow \pi^+\pi^- J/\psi (J/\psi \rightarrow \gamma p\bar{p})$ events that satisfy the $\gamma p\bar{p}$ selection criteria. The smooth curves are the results of the fit described in the text.

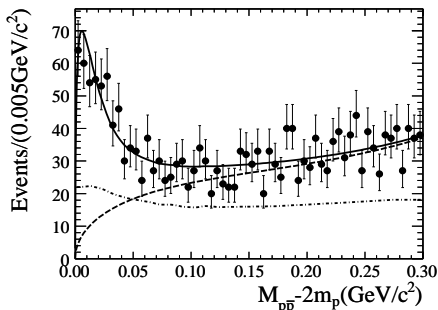


FIG. 3: The $p\bar{p}$ invariant mass spectrum for the $\psi' \rightarrow \pi^+\pi^- J/\psi (J/\psi \rightarrow \gamma p\bar{p})$ after final event selection. The solid curve is the fit result; the dashed curve shows the fitted background function, and the dash-dotted curve indicates how the acceptance varies with $p\bar{p}$ invariant mass.

tribution is well described by a function of the form $f_{bkg}(\delta) = N(\delta^{1/2} + a_1\delta^{3/2} + a_2\delta^{5/2})$, where $\delta = M_{p\bar{p}} - 2m_p$ and the shape parameters a_1 and a_2 are determined from a fit to selected $\gamma p\bar{p}$ events for $\psi' \rightarrow \pi^+\pi^- J/\psi (J/\psi \rightarrow \gamma p\bar{p})$ phase-space MC sample shown in Fig. 2(b).

To characterize the $p\bar{p}$ threshold mass enhancement, we fit it with an acceptance weighted Breit-Wigner (BW) function of the form $BW(M) \propto \frac{q^{2L+1}k^3}{(M^2 - M_0^2)^2 + M_0^2\Gamma^2}$, where Γ is a constant (determined from fit), q is the proton momentum in the $p\bar{p}$ rest-frame, L is the $p\bar{p}$ orbital angular momentum, and k is the photon momentum, together with the function $f_{bkg}(\delta)$ with free normalization and constants a_1 and a_2 fixed at the $\pi^0 p\bar{p}$ phase-space MC values (*i.e.* the curves shown in Fig. 2) to represent the background from mis-reconstructed $\pi^0 p\bar{p}$ events and a possible non-resonant $p\bar{p}$ phase-space contribution. The BW is multiplied by the MC-determined signal acceptance that is corrected for MC and data differences of the low momentum π^+ and π^- tracking efficiencies. The tracking efficiencies determined from data are measured using samples of tagged protons and antiprotons from the process $J/\psi \rightarrow p\bar{p}\pi^+\pi^-$.

The result of a fit using $L = 0$ and confined to the

$M_{p\bar{p}} - 2m_p < 0.3 \text{ GeV}/c^2$ mass region is shown in Fig. 3. The fit returns a signal yield of 519^{+36}_{-39} (stat), a peak mass of $M = 1861^{+6}_{-13}$ (stat) MeV/c^2 and a width of $\Gamma = 0 \pm 23 \text{ MeV}/c^2$. The fit quality is $\chi^2/d.o.f. = 42.6/56$.

In the above-described fit, the phase-space contribution is treated as an incoherent background under the enhancement. Possible fitting biases near threshold are investigated using a set of MC samples that combine the signal with a uniform incoherent phase-space background. In each MC sample, the mass, width, and number of signal events are obtained from a fit using the same procedure as that done on the data. The averaged differences between the fitted output and input values are taken as a systematic uncertainty associated with a possible fitting bias. The r.m.s. of each parameter's bias measurements is taken as the statistical error. The systematic uncertainties found from varying the bin size and the fitting range are also included. The total systematic error on the mass is $^{+7}_{-26} \text{ MeV}/c^2$. Including the systematic error, the upper limit on the width is $\Gamma < 38 \text{ MeV}/c^2$ at a 90% confidence level.

We also tried to fit the $p\bar{p}$ mass spectrum using known particle resonances to represent the low-mass peak. There are two spin-zero resonances listed in the PDG tables in this mass region: the $\eta(1760)$ with $M_{\eta(1760)} = 1756 \pm 9 \text{ MeV}/c^2$ and $\Gamma_{\eta(1760)} = 96 \pm 70 \text{ MeV}/c^2$, and the $\pi(1800)$ with $M_{\pi(1800)} = 1816 \pm 14 \text{ MeV}/c^2$ and $\Gamma_{\pi(1800)} = 208 \pm 12 \text{ MeV}/c^2$. A fit with f_{bkg} and an acceptance-weighted S -wave BW function with mass and width fixed at the PDG values for the $\eta(1760)$ produces $\chi^2/d.o.f. = 144.8/56$; and using the $\pi(1800)$ parameters produces $\chi^2/d.o.f. = 161.7/56$.

In summary, an anomalous strong, near-threshold enhancement in the $p\bar{p}$ invariant mass distribution is observed in the decay process of $\psi' \rightarrow \pi^+\pi^- J/\psi (J/\psi \rightarrow \gamma p\bar{p})$. If it is fitted with an S -wave Breit-Wigner resonance function, the peak mass is $M = 1861^{+6}_{-13}$ (stat) $^{+7}_{-26}$ (syst) MeV/c^2 and the width is $\Gamma < 38 \text{ MeV}/c^2$ at the 90% confidence level. These values are consistent with the published BESII results [1]. As indicated in Ref. [19], the $p\bar{p}$ mass threshold enhancement may also be fitted with a broad structure ($\Gamma \sim 100 \text{ MeV}/c^2$) multiplied by an FSI factor in Ref. [12]. More precise measurement of the shape of the $p\bar{p}$ mass threshold enhancement and more sophisticated fits such as including some model dependent FSI factor in the fit will be performed with much higher statistics J/ψ data sample collected at BESIII.

The BESIII collaboration thanks the staff of BEPCII and the computing center for their hard efforts. This work is supported in part by the Ministry of Science and Technology of China under Contract No. 2009CB825200; National Natural Science Foundation of China (NSFC) under Contracts Nos. 10625524, 10821063, 10825524, 10835001, 10935007; the Chinese Academy of Sciences (CAS) Large-Scale Scientific Facility Program; CAS un-

der Contracts Nos. KJCX2-YW-N29, KJCX2-YW-N45; 100 Talents Program of CAS; Istituto Nazionale di Fisica Nucleare, Italy; Russian Foundation for Basic Research under Contracts Nos. 08-02-92221, 08-02-92200-NSFC-a; Siberian Branch of Russian Academy of Science, joint project No 32 with CAS; the Chinese University of Hong Kong Focused Investment Grant under Contract No.

3110031; U. S. Department of Energy under Contracts Nos. DE-FG02-04ER41291, DE-FG02-91ER40682, DE-FG02-94ER40823; WCU Program of National Research Foundation of Korea under Contract No. R32-2008-000-10155-0. D. Cronin-Hennessy thanks the A.P. Sloan Foundation.

-
- [1] BES Collaboration, J.Z. Bai *et al.*, Phys. Rev. Lett. **91**, 022001 (2003).
- [2] M.Z. Wang *et al.*, Phys. Rev. Lett. **92**, 131801 (2004).
- [3] S. Jin, invited plenary talk at the XXXIIth International Conference on High Energy Physics (ICHEP04), Beijing, 2004.
- [4] BES Collaboration, M. Ablikim *et al.*, Phys. Rev. Lett. **99**, 011802 (2007).
- [5] CLEO Collaboration, S.B. Athar *et al.*, Phys. Rev. **D 73**, 032001 (2006).
- [6] BES Collaboration, M. Ablikim *et al.*, Eur. Phys. J. **C53**, 15, (2008).
- [7] A. Datta and P.J. O'Donnell, Phys. Lett. **B567**, 273 (2003); M.L. Yan *et al.*, Phys. Rev. **D 72**, 034027 (2005); B. Loiseau and S. Wycech, Phys. Rev. **C72**, 011001 (2005).
- [8] J. Ellis, Y. Frishman and M. Karliner, Phys. Lett. **B566**, 201 (2003); J.L. Rosner, Phys. Rev. **D 68**, 014004 (2003).
- [9] C.S. Gao and S.L. Zhu, Commun. Theor. Phys. **42**,844(2004), hep-ph/0308205.
- [10] G.J. Ding and M.L. Yan, Phys. Rev. **C 72**, 015208 (2005).
- [11] B.S. Zou and H.C. Chiang, Phys. Rev. **D 69**, 034004 (2003).
- [12] A. Sibirtsev *et al.*, Phys. Rev. **D 71**, 054010 (2005).
- [13] I.S. Shapiro, Phys. Rep. **35**, 129 (1978); C.B. Dover and M. Goldhaber, Phys. Rev. **D 15**, 1997 (1977).
- [14] E. Klempt *et al.*, Phys. Rep. **368**, 119 (2002); J.-M. Richard, Nucl. Phys. Proc. Suppl. **86**, 361 (2001).
- [15] BESIII Collaboration, M. Ablikim *et al.*, Design and construction of the BESIII detector, arXiv:0911.4960, accepted by Nucl. Instrum. Meth. **A**.
- [16] BES Collaboration, J. Z. Bai *et al.*, Nucl. Instrum. Meth. **A 344**, 319 (1994); Nucl. Instrum. Meth. **A 458**, 627 (2001).
- [17] J.C. Chen *et al.*, Phys. Rev. **D 62**, 034003 (2000).
- [18] Particle Data Group, C. Amsler *et al.*, Phys. Lett. **B667**, 1 (2008).
- [19] BES Collaboration, M. Ablikim *et al.*, Phys. Rev. Lett. **95**, 262001 (2005).